ELSEVIER

Journal of Alloys and Compounds 419 (2006) 227–233

Journal of ALLOYS AND COMPOUNDS

www.elsevier.com/locate/jallcom

Self-propagating high-temperature synthesis of TiC–WC composite materials

M.J. Mas-Guindal [a,*], L. Contreras [a], X. Turrillas [b], G.B.M. Vaughan [c], Å. Kvick [c], M.A. Rodríguez [a]

[a] *Instituto de Cerámica y Vidrio, CSIC, C/Kelsen, No 5, 28049 Madrid, Spain*
[b] *Eduardo Torroja Institute for Construction Sciences, CSIC, 28033 Madrid, Spain*
[c] *European Synchrotron Radiation Facility, 38043 Grenoble, France*

Received 7 July 2005; accepted 22 August 2005
Available online 18 November 2005

Abstract

TiC–WC composites have been obtained in situ by self-propagating high-temperature synthesis (SHS) from a mixture of compacted powders of elemental titanium, tungsten and graphite. The Rietveld method has proved to be a useful tool to quantify the different phases in the reaction and calculate the cell parameters of the solid solution found in the products. The reaction has also been followed in real time by X-ray diffraction at the European Synchrotron Radiation Facility (ESRF ID-11 Materials Science Beamline). The mechanism of the reaction is discussed in terms of the diffusion of liquid titanium to yield titanium carbide with a solid solution of tungsten. The microstructures of the materials obtained by this method are presented.

Keywords: Self-propagating high-temperature synthesis; Combustion synthesis; Synchrotron radiation; X-ray diffraction; Carbides

1. Introduction

In this paper, the TiC–WC system is being discussed; characteristic of this system is the high hardness of its components (TiC has 31 GPa Vickers hardness and WC has 25 GPa), which facilitates its uses as abrasives and cutting and polishing tools among others [1,2]. Metcalfe was the first to report a study on this system [3]. The phase diagram at low temperature shows the existence of two main regions (Fig. 1): under 45 mol% of WC a solid solution of (Ti,W)C is formed, in which titanium atoms of the TiC fcc cubic cell are substituted by tungsten atoms. If more than 45 mol% of WC is present, two phases appear: the solid solution and a phase only formed by hexagonal WC. When temperature is above 1600 °C an increase in the degree of solid solution is observed and more tungsten is accepted in solid solution before the appearance of the two phases [4,5].

The self-propagating high-temperature synthesis (SHS) is a technique that has proved to be very useful to obtain metallic, ceramic and composite materials with hardness and refractoriness that make them useful as abrasives, cutting tools, armour of vehicles, thermal barriers, etc. Among these compounds there are borides, carbides, carbonitrides, hydrides, nitrides, silicides and others. The reaction is characterised by a high exothermicity which leads to a self-sustained process. Ignition is usually produced by means of an electric or calorific device and combustion front propagation is made at high speeds (1–100 mm/s), favoured if powders are compacted. As advantages we could mention the low energetic cost, its productivity or the high yields obtained [1,6–11].

The objective is to develop a way of predicting the solid solution degree by the calculation of the unit cell parameters and study the phase percentages obtained when different compositions of TiC–WC are prepared by means of SHS. Reactions to be studied are:

$$4Ti + 5C + W \rightarrow 4TiC + WC \quad (I)$$

$$3Ti + 4C + W \rightarrow 3TiC + WC \quad (II)$$

$$2Ti + 3C + W \rightarrow 2TiC + WC \quad (III)$$

* Corresponding author. Tel.: +34 91 7355840; fax: +34 91 7355843/45.
E-mail address: mjmg@icv.csic.es (M.J. Mas-Guindal).

0925-8388/$ – see front matter © 2005 Elsevier B.V. All rights reserved.
doi:10.1016/j.jallcom.2005.08.079

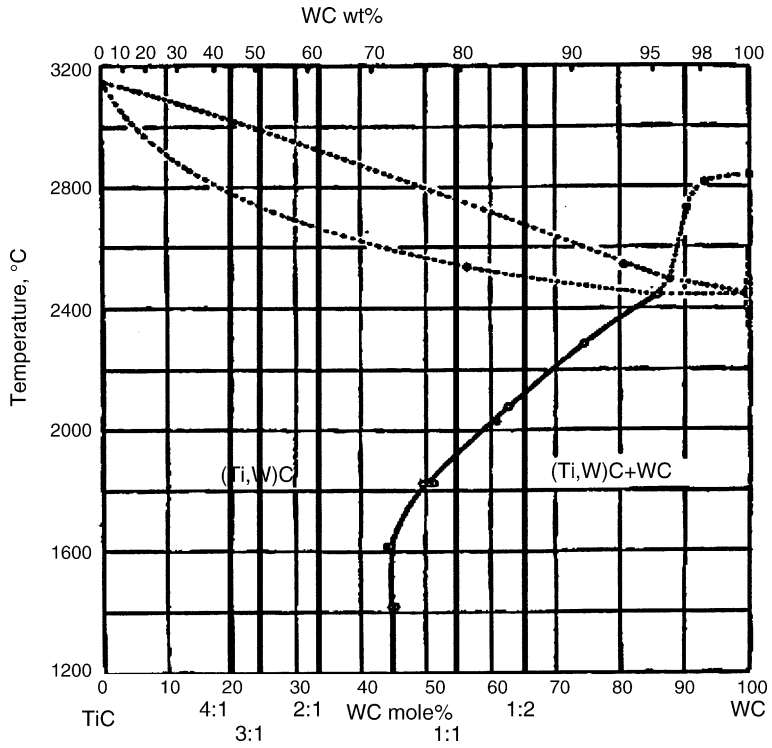

Fig. 1. Binary phase diagram for TiC–WC system (6). Vertical gross lines indicate the localization of the different reactions in the diagram.

$$\mathrm{Ti} + 2\mathrm{C} + \mathrm{W} \rightarrow \mathrm{TiC} + \mathrm{WC} \quad \text{(IV)}$$

$$\mathrm{Ti} + 3\mathrm{C} + 2\mathrm{W} \rightarrow \mathrm{TiC} + 2\mathrm{WC} \quad \text{(V)}$$

Also reaction of pure titanium with graphite to give titanium carbide was studied as a reference. Additional work has been done using Synchrotron Radiation to try to explain the mechanism of the combustion.

It has been empirically established that when the adiabatic temperature (T_{ad}) is lower than 1800 K, reactions are not self-sustained [6]. Calculation of T_{ad} can be done by solving the equation, which comes from the definition of heat capacity [12]:

$$\Delta H = \Delta H_{r,T_0} + \int_{T_0}^{T_{ad}} C_p(\text{products})\,dT$$

where ΔH is the reaction enthalpy, $\Delta H_{r,T_0}$ is the enthalpy at T_0 (initial temperature, normally 298 K) and C_p (products) is the heat capacity for the products of the reaction. If the system is adiabatic, then:

$$-\Delta H_{r,T_0} = \int_{T_0}^{T_{ad}} C_p(\text{products})\,dT$$

Using data taken from bibliography [13] and summarised in Table 1 we find that all reactions proposed can be self-sustaining; however, reaction (V) will have trouble to be self-sustaining for its T_{ad} is below the limit. It is also seen that pure tungsten carbide formation is not self-sustaining (T_{ad} = 1000 K). On the other hand, pure titanium carbide has a very favoured reaction, as expected by its high T_{ad} (3200 K). Thus another advantage of mixing both, titanium and tungsten with carbon, is that titanium carbide formation acts as a sort of chemical activator for obtaining tungsten carbide by SHS.

The high temperatures reached and the high speeds of combustion front propagation make these reactions difficult to follow, so little knowledge about the mechanism or kinetics is available. Time resolved X-ray diffraction (TRXRD) using high intensity synchrotron radiation has proved to be very useful for

Table 1
Thermodynamic data for basic substances [13]

Substance	Melting point (°C)	ΔH°_{298} (J/mol)	C_p (J/mol K)[a]			
			A	*B*	*C*	*D*
Ti	1941	0.0	17.834	24.376	3.047	−8.840
W	3680	0.0	19.304	20.710	0.385	−18.086
C (graphite)	3820	0.0	−7.094	59.154	0.799	−32.718
TiC	3290	−184,568.0	−97.045	667.897	4.587	−826.766
WC	3058	−40,180.8	43.391	8.639	−9.321	−1.021

[a] $C_p = A + B \times 10^{-3}\,T + C \times 10^{5}\,T^{2} + D \times 10^{-6}\,T^{2}$.

in situ following of the reaction [9–11]. For this part of the work, the Materials Science Beamline (ID11) at the European Synchrotron Radiation Facility (ESRF) in Grenoble, France, has been used as a complement to study reaction (I).

Finally, the Rietveld refinement method [14] for quantitative phase analysis has been used in diffractograms recorded with conventional X-ray diffraction to obtain the phase percentage of the products and refine the cell parameters in order to obtain the degree of solid solution [15].

2. Experimental procedure

2.1. Powder preparation

The following starting materials have been used: (a) pure Ti powder >99% (William Rowland Ltd., UK) with particle size $d_{50} = 84$ μm, (b) graphite powder 99.6% (Sofacel, Spain) with particle size $d_{50} = 1.7$ μm, (c) pure W powder (William Rowland Ltd., UK) with particle size $d_{50} = 1.2$ μm.

Also, an extra amount of Ti + C was weighted, in the same proportion given, in order to use it as an ignitor of combustion (this way it supplies the necessary energy for the starting of the reaction).

Powders were mixed in an agata mortar and pressed in a 30-mm diameter stainless steel die. A pressure of 2 MPa was applied to obtain 15 mm thickness cylindrical pellets.

2.2. Post-reaction study

Reactions were made in a SHS reactor and triggered in argon atmosphere using a tungsten wire and titanium–graphite powder as bed reaction. Pellets with composition (IV) had to be almost fully covered with the Ti–C powder in order to make reaction possible. Reaction (V) did not start because of its very low T_{ad}.

2.3. Real-time study

The ESRF ID-11 Materials Science Beamline was used. Pressed-powder was placed between the X-ray source ($\lambda = 0.26102$ Å) and the detector on a graphite sample-holder, which was adjusted so that the beam hit the centre of the sample (0.2 mm × 0.2 mm). The diffracted photons, within a 15° 2θ cone, obtained by transmission, were collected with a Frelon CCD camera.

Initiating current was fed through the wire a few seconds before starting the XRD acquisition. The experiment was conducted in air atmosphere. More details of the experiment are found in [11].

Exposure time per frame was 35 ms and the total readout data storage time was 30 ms, rendering a total time resolution of 65 ms per frame. During each experiment 600 XRD frames were recorded successively by a workstation running under LINUX with Spec [16] acting as software for control and data acquisition.

2.4. SEM

Porous specimens were embedded in an epoxy resin under vacuum. Polishing was made on a lapping disk with diamond paste up to a degree of 1 μm The polished surface was cleaned with isopropilic alcohol, dried and coated with gold by sputtering. Then, it was observed by SEM with a Zeiss DSM-950 microscope (including EDS analysis).

2.5. XRD

Products were ground and sieved below 60 μm size for DRX. Powders were mixed with 20% Si-NIST used as an internal standard. Recording of the data was made in a Siemens Diffraktometer D5000 ($K_{Cu\alpha} \rightarrow \lambda = 1.54056$ Å) with a program to ensure quality of data. The range was from 20 to 80° at a step rate of 0.03° and an acquisition time of 22 s for each step. The diffractometer optic used to collect the samples was: a fixed aperture slit of 2 mm, one scattered-radiation slit of 2 mm after the sample, followed by a system of secondary Soller slits and the reception slit of 0.2 mm. After that secondary curved graphite monochromator is placed and finally the detector slit of 0.6 mm.

2.6. Data processing

The frames collected at the ESRF containing diffraction rings were integrated using scripts developed at ID11 around the Fit2D program [17]. Information of each frame was condensed into a standard format containing, 2θ, intensity and statistical error for every step. Further treatment of the XRD patterns was made with a series of scripts written in IDL [18] to fit diffraction peaks to Gaussian curves. Transform [19] was used to map the diffraction pattern sequence. Rietveld analysis was made using Fullprof Suite [20].

3. Results and discussion

3.1. Post-synthesis study

Here, the obtained results from the reactions made at the laboratory will be briefly described.

3.1.1. TiC

As expected, Rietveld analysis shows that mostly TiC is present, together with some unreacted elemental titanium and graphite. Table 2 shows the phase percentages obtained for all the reactions. Fig. 2(a) shows the adjusted diffractogram with phases indicated by Bragg peaks' positions.

3.1.2. 4TiC:1WC

It can be seen in Table 2, that a 67% of solid solution with formula $Ti_{0.8}W_{0.2}C$ (correlating well with phase equilibrium diagram prediction) is detected. There is also presence of titanium carbide without tungsten (18%) and ca. 12% of unreacted mixture and WC.

3.1.3. 3TiC:1WC

Although there is still a majority of solid solution (with approximate formula $Ti_{0.75}W_{0.25}C$), very little impurities have been detected (WC and W_2C) and there is no titanium carbide without solid solution, but there is little presence of unreacted titanium, tungsten and graphite. SEM study (Fig. 3(a)) confirms the data by showing the presence of two main zones: a majoritarian darker one, which corresponds to the solid solution, and a lighter one which corresponds particularly to the unreacted mixture (ca. 18% of product).

Table 2
Phase percentages obtained for each of the reactions

	TiC	4TiC:1WC	3TiC:1WC	2TiC:1WC	1TiC:1WC
%(Ti,W)C		67.00	78.63	52.76	25.92
%TiC	78.60	17.97			
%WC		2.71	3.36	12.33	39.91
%W_2C			0.69	2.92	14.41
%W		4.00	5.57	11.91	4.03
%C	11.42	3.39	2.39	3.80	4.87
%Ti	9.98	4.00	9.36	13.28	10.86

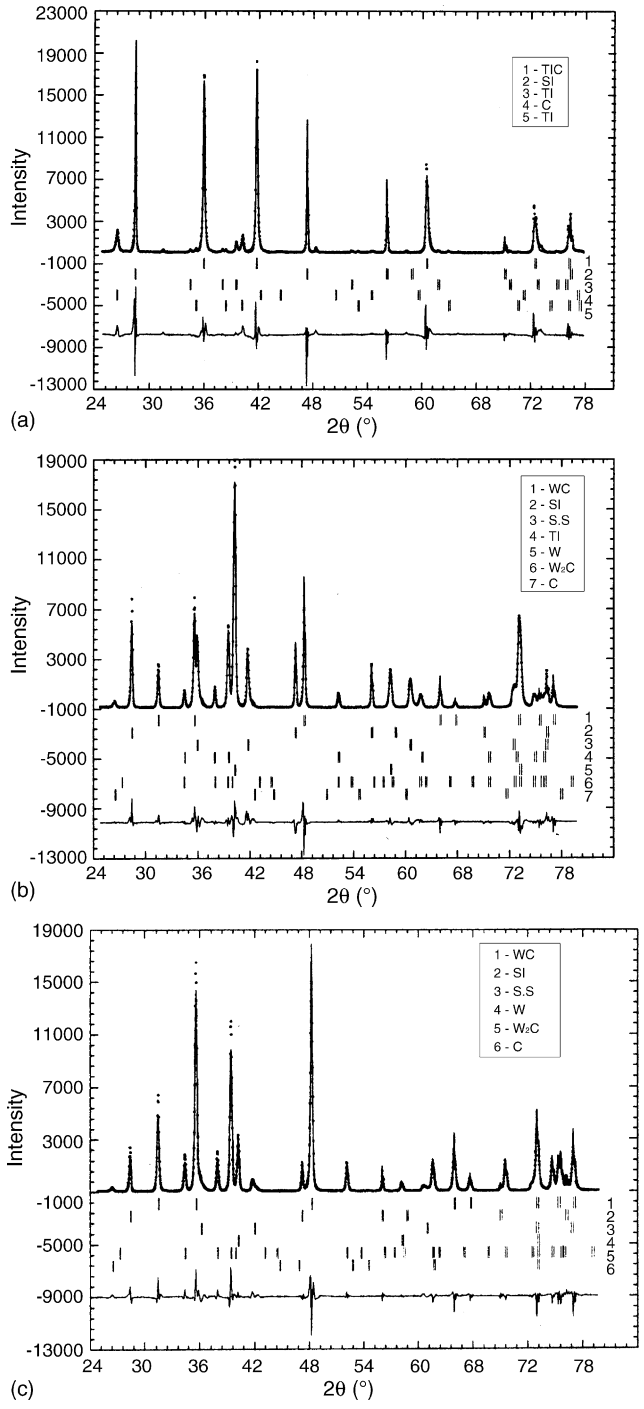

Fig. 2. Selected adjusted diffractograms for reaction products; dotted line corresponds to observed data and continuous line to calculated data; Bragg positions are indicated with vertical lines under each peak and it is also shown the difference curve. (a) Diffractogram of TiC obtention ($R_p = 24.2$, $R_{wp} = 31.2$, $R_e = 4.73$, $\chi^2 = 43.4$); (b) diffractogram of reaction (III) ($R_p = 13.8$, $R_{wp} = 17.5$, $R_e = 4.05$, $\chi^2 = 18.7$); (c) diffractogram of reaction (IV) ($R_p = 13.5$, $R_{wp} = 17.0$, $R_e = 15.2$, $\chi^2 = 1.3$).

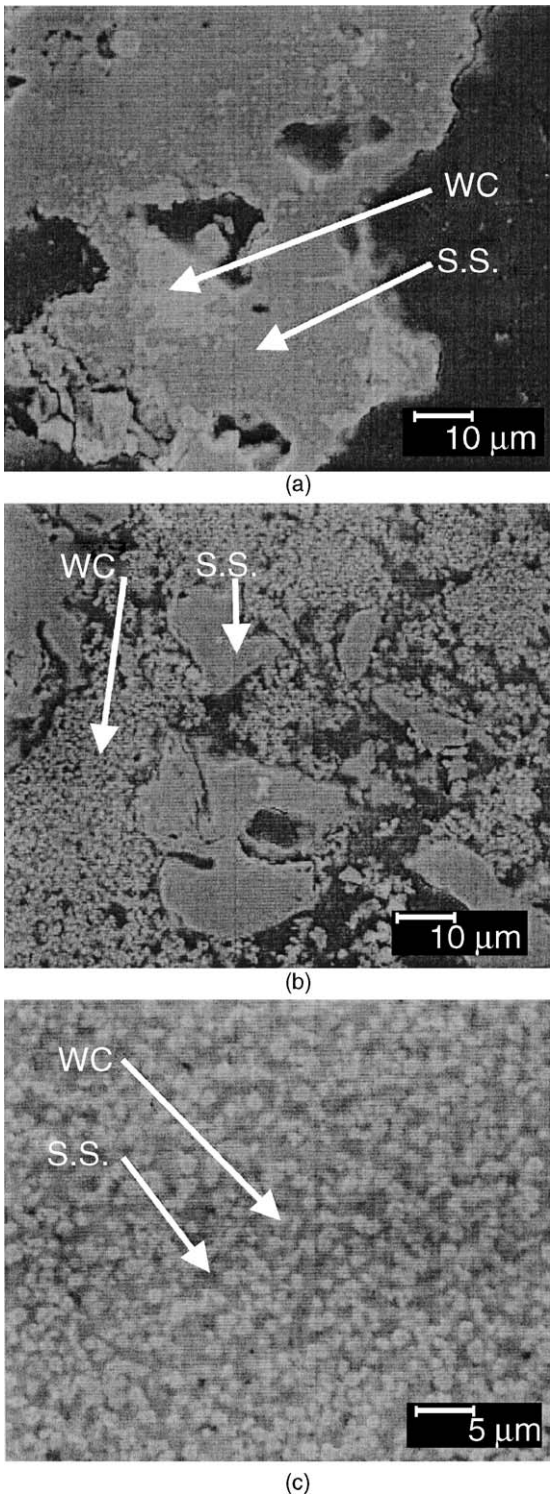

Fig. 3. SEM Micrographs of different reactions: (a) reaction (II), (b) reaction (IV), (c) reaction (IV). Zoom on the light phase showing the micrometrical spheres.

3.1.4. 2TiC:1WC

The solid solution percentage appears decreased to a 52% of the total product; its formula is $Ti_{0.67}W_{0.33}C$. An increase on the amount of unreacted mixture to a 30% level is observed and up to 11% of WC is found; Fig. 2(b) shows the diffractogram with Bragg-peaks' positions and Rietveld refinement. SEM-microstructure is similar as that of previous reaction but with an increase in the lighter zone percentage, corresponding to the unreacted mixture.

Table 3
Cell parameters and solid solution degree

Composition	S.S. degree	$a=b=c$
TiC	TiC	4.3280
4TiC:1WC	$Ti_{0.8}W_{0.2}C$	4.3260
3TiC:1WC	$Ti_{0.75}W_{0.25}C$	4.3247
2TiC:1WC	$Ti_{0.65}W_{0.35}C$	4.3235
1TiC:1WC	$Ti_{0.60}W_{0.40}C$	4.3227

3.1.5. TiC:WC

The most abundant phase corresponds now to WC (40%) and solid solution percentage has decreased to 26%; its formula is $Ti_{0.55}W_{0.45}C$ which corresponds to saturation of the solid solution.

It is clearly seen an increase in the amount of W_2C to a 14% and the unreacted mixture percentage is a 20%. Fig. 2(c) shows the diffractogram. Micrograph in Fig. 3(b) shows the existence of a mostly light phase corresponding to WC and a darker one, which is the remainder. A zoom on the light phase (Fig. 3(c)) shows that WC has a microstructure of little spheres of micrometric size (ca. 1.5 μm).

3.1.6. Discussion

Table 3 shows the unit cell parameters and the degree of solid solution found using the Rietveld method. Results are in good agreement with expected behaviour, i.e. the more tungsten entering in solid solution within the titanium carbide cell, a reduction in the unit cell is observed. This can be explained by the atomic radii of atomic elements: tungsten radium is 1.41 Å and titanium radium is 1.47 Å, and a substitution of titanium atoms by tungsten atoms will thus result in a decrease of the cell and a displacement of the peaks corresponding to solid solution to a higher angle in the difrractogram.

A graphic representation of cell parameter versus solid solution degree (Fig. 4) shows that it fits a linear model indicating that Vegard's Law for solid solutions is being followed [21]. The equation for this model is:

$$Y = 4.32805 - 1.29803 \times 10^{-4} X \quad \text{(IX)}$$

Y being the cell parameter and X the amount of tungsten in solid solution (takes values between 0 and 0.45).

This expression, then, can be used for predicting the approximate solid solution degree found in any final proportion between TiC and WC of this system.

The presence of secondary phases and rests of reactants in the product pellets is noticeable. There are various explanations for this. Mainly, it is due to the lack of equilibrium during the reaction: rapid heating and cooling of the sample makes it difficult to reach the equilibrium; as reactions happen at high speed and intermediate species, like W_2C (which should not be stable below 1300 °C [22,23]), don't evolve to the desired products and remain intact. Due to the small size of the pellets, which implies a bigger percentage of powder exposed to the atmosphere, there is an increase in non-desired products, specially at the surface of pellets. This is the case of the tungsten oxide that appears in the reaction at the synchrotron. A secondary effect of the lack of equilibrium is that reacting agents do not react completely; therefore, they appear in the final product.

3.2. Real-time study

3.2.1. Synchrotron results

Fig. 5 shows diffractograms of reaction (I) obtained at the laboratory and the synchrotron. Data have been converted to d^{-1} (nm^{-1}) for ease of comparison. The first impression shows that the synchrotron product is far cleaner from impurities and non-reacted parts than the laboratory obtained one; this happens not only because of the better precision that synchrotron radiation generates, but also from the fact that at the synchrotron measure is made on only one spot of the pellet, while for normal DRX, the product has suffered a milling and sieving process that introduces some impurities as a larger part of the pellet is used during the milling. Synchrotron peaks are assigned mainly to solid solution; nevertheless, solid solution and titanium carbide have a similar pattern, and in the case of the synchrotron the lack of significant peaks for WC or W_2C leads to supposition that most of the tungsten is present in the solid solution, as expected for that composition. One can also observe the presence of non-reacted graphite and a small peak at $d^{-1} = 4.5$, which

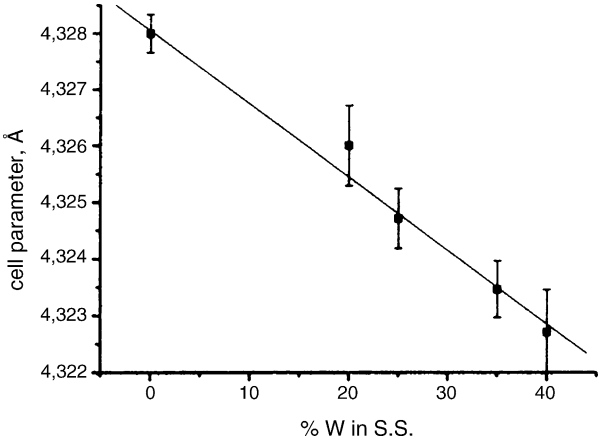

Fig. 4. Representation of cell parameter vs. solid solution degree and result of linear fitting of the dots.

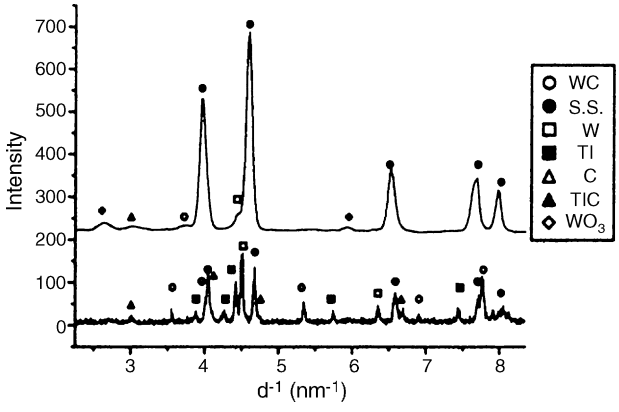

Fig. 5. Comparative among the diffractogram of reaction 4:1 made at laboratory (down) and at the synchrotron (up).

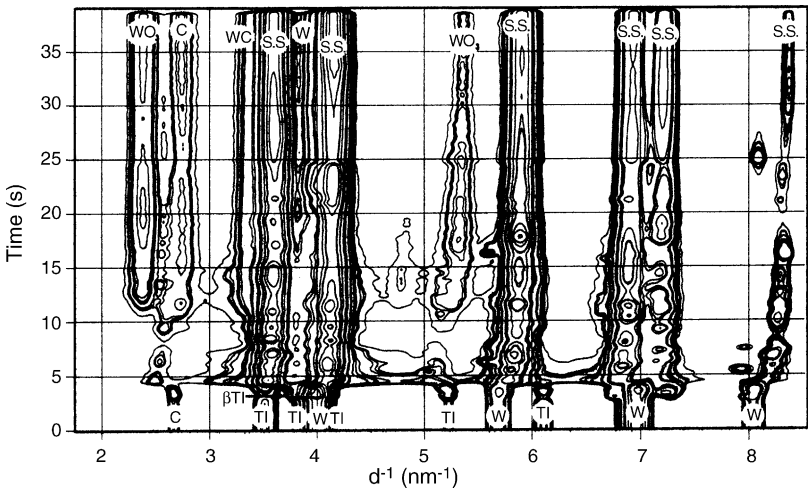

Fig. 6. Contour map of reaction; main peaks have labels identifying them.

could correspond to non-reacted tungsten. Peak at $d^{-1} = 2.6$ corresponds to tungsten oxide, which appears only at the surface of the pellet because of the contact with air.

3.3. Reaction mechanism

Four main stages are seen: heating, transformation of α-titanium into β-titanium, reaction and cooling. Collected diffractograms provide a map of the reaction; it is worth noting that reaction happens rapidly after the preheating of reactants. A contour bidimensional map of the reaction shows the evolution of the different phases during the process (Fig. 6) and is helpful in visualising the mechanism, explained next. Selected diffractograms of the depicted stages are found in Fig. 7:

- Initial situation at $t = 0$ s shows the peaks corresponding to α-titanium, tungsten and graphite.
- At about 2.5 s, the transformation of α-titanium (hexagonal-P63/mmc) into (β-titanium (bcc-Fm3m) starts. At $t = 3.25$, peak at $d^{-1} = 4.3$, corresponding to cubic titanium reaches the highest intensity and a moment later peaks decrease presumably due to appearance of liquid titanium, but no evidence is shown.
- Titanium (supposedly in liquid state) diffuses at ca. $t = 4.0$ s through the graphite and starts the reaction. The diffractogram at about 4.62 s shows peaks corresponding to the conversion of the elements into the products; at that time, also the reaction of tungsten into solid solution can be observed, as tungsten's main peak at $d^{-1} = 4.46$ disappears. At 6 s, an increase

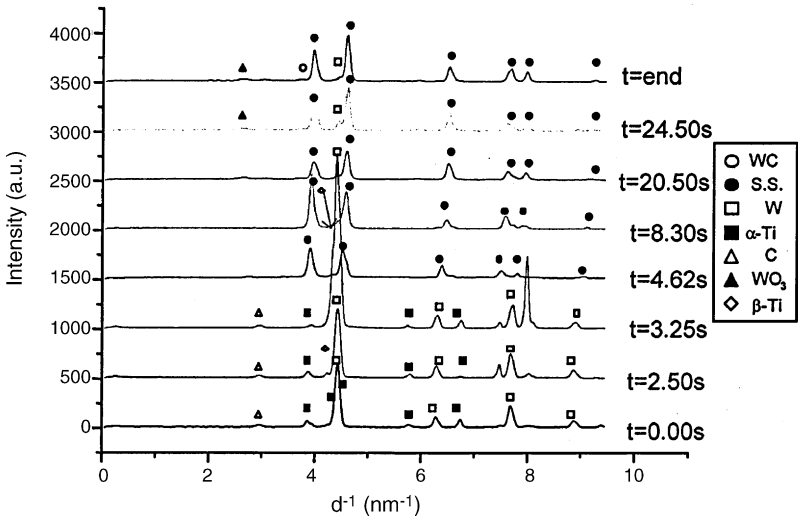

Fig. 7. Diffractograms acquired with synchrotron radiation during reaction and representative of each stage:
$t = 0$ s, raw products.
$t = 2.5$ s, starting of transformation of α-titanium to β-titanium.
$t = 3.25$ s, maximum intensity of β-titanium peak at $d^{-1} = 4.3$.
$t = 4.62$ s, start of appearance of products.
$t = 8.3$ s, reaction starts to cool.
$t = 20.5$ s, principal phases already formed.
$t = 24.5$ s, at the medium of cooling, product is already formed.
Diffractogram corresponding to final cooled product.

of some of the peaks corresponding to the products can be observed.
- The process starts cooling at about 8.3 s from the initial moment. From now on no special additional features are observed. The main characteristic of this stage is the consolidation of the solid solution phase with the growing of solid solution peaks and the solidification of the molten substances. The presence of W_2C is also detected, but at 20 s it transforms into product and does not appear in the final diffractogram.
- At about 14 s, one observes the appearance of peaks corresponding to tungsten oxide, (mainly WO_3); which, as already mentioned, is an effect that happens only at the surface of the pellet.
- Cooling after this time does not add new noticeable reactions as can be seen at 20.5 s, 24.5 s and the final diffractogram.

Summing up, reaction passes through the transformation of α-titanium into β-titanium and then into liquid, so that it diffuses through the sample. Formation of products starts just after the melting of reactants (about 5 s after starting).

4. Conclusions

- A hard composite material made of a mixed carbide of titanium and tungsten has been obtained by means of a SHS reaction using as reagents the elemental forms.
- The speed of the SHS reaction implies that no complete equilibrium state is achieved during reaction and secondary phases appear diminishing purity.
- The Rietveld method has been used successfully to develop an expression which permits us to have a quite accurate measure of the cell parameter of the solid solution formed in the mixed carbide; insertion of tungsten into the titanium carbide cell results in a linear evolution of the unit cell parametre, according to Vegard's Law for solid solutions. Its expression is:

$$Y = 4.32805 - 1.29803 \times 10^{-4} X$$

for X between 0 and 0.45. Cell parameter decreases with the introduction of tungsten.
- If more than 45% of tungsten is present, two phases occur: saturated solid solution ($Ti_{0.55}W_{0.45}C$) and pure tungsten carbide.
- The percentage of solid solution formation decreases when there is more tungsten in the reaction and results in more amount of reactants in the final product.
- Coexistence of phases starts to appear when going near the saturation of solid solution. The solid solution percentage decreases markedly when entering the two-phase zone and an increase in tungsten carbide percentage is observed.
- The reaction mechanism probably occurs through the diffusion of liquid titanium into the graphite and the tungsten forming titanium carbide first, and then entering tungsten into this formed carbide.

Acknowledgments

We thank the ESRF for beamtime granted through experiment CH-1235. This work has been supported by the Spanish Science and Technology Agency (CICYT) under project No. MAT 2004-04923-C02-01.

References

[1] A.G. Merzhanov, Ceram. Int. 21 (1995) 371–379.
[2] M. Pidria, E. Merlone, M. Rostagno, L. Tabone, F. Bechis, D. Vallauri, F.A. Deorsola, I. Amato, M.A. Rodríguez, Mater. Sci. Forum 432 (2003) 4374–4378.
[3] A.G. Metcalfe, J. Ins. Met. 73 (1947) 591–607.
[4] S. Johnsson, Z. Metallkd. 87 (10) (1996) 788.
[5] A. Saidi, M. Barati, J. Mater. Prod. Tec. 124 (2002) 166–170.
[6] Z.A. Munir, U. Anselmi-Tamburini, Mater. Sci. Rep. 3 (7–8) (1989) 277–365.
[7] M.A. Rodríguez, N.S. Makhonin, J.A. Escriña, I.P. Borovinskaya, M.I. Osendi, M.F. Barba, J.E. Iglesias, J.S. Moya, Adv. Mater. 7 (8) (1995) 745–747.
[8] J.S. Moya, J.E. Iglesias, F.J. Limpo, J.A. Escriña, N.S. Makhonin, M.A. Rodríguez, Acta Mater. 45 (8) (1997) 3089–3094.
[9] C. Curfs, I.G. Cano, G.B.M. Vaughan, X. Turrillas, Å. Kvick, M.A. Rodríguez, J. Eur. Ceram. Soc. 22 (2002) 1039–1044.
[10] L. Contreras, X. Turrillas, G.B.M. Vaughan, Å. Kvick, M.A. Rodríguez, Acta Mater. 52 (2004) 4783–4790.
[11] L. Contreras, X. Turrillas, M.J. Mas-Guindal, G.B.M. Vaughan, Å. Kvick, M.A. Rodríguez, J. Solid State Chem. 178 (2005) 1595–1600.
[12] C.R. Bowen, D. Derby, Br. Ceram. Trans. 96 (1) (1997) 25.
[13] HSC CHEMISTRY 5.11 ©Outokumpu Research Oy, Pori, Finland, A. Roine www.outokumpu.com/hsc.
[14] H.M. Rietveld, J. Appl. Cryst. 2 (1969) 65–71.
[15] L.B. McCusker, R.B. Von Dreele, D.E. Cox, D. Louër, P. Scardi, J. Appl. Cryst. 32 (1999) 36.
[16] SPEC, Certified Scientific Software, P.O. BOX 390640, Cambridge, MA 02139.
[17] A. Hammersley, S.O. Svensson, A. Thompson, Nucl. Instrum. Methods A346 (1994) 312–321.
[18] Research Systems Inc. (Kodak Company), Sterling, VA 20164, USA. Program IDL Version 5.2 (1998) www.rsinc.com.
[19] Research Systems Inc. (Kodak Company), Sterling, VA 20164, USA. Program NOeSYS. Version 1.2 (1998) www.rsinc.com.
[20] T. Roisnel, J. Rodríguez-Carvajal, FullProf Suite (May 2003) http://www.llb.cea.fr/fullweb/winplotr/winplotr.htm.
[21] L. Vegard, Z. Phys. 5 (1921) 17.
[22] G. Jiang, W. Li, H. Zhuang, Mater. Sci. Eng. A354 (2003) 351–357.
[23] G. Jiang, H. Zhuang, W. Li, Ceram. Int. 30 (2004) 191–197.